SUV Varies with Time After Injection in ^{18}F-FDG PET of Breast Cancer: Characterization and Method to Adjust for Time Differences

Sylvain Beaulieu, MD; Paul Kinahan, PhD; Jeffrey Tseng, MD; Lisa K. Dunnwald, BS; Erin K. Schubert, BS; Pam Pham, BS; Barbara Lewellen, BS; and David A. Mankoff, MD, PhD

Division of Nuclear Medicine, University of Washington Medical Center, Seattle, Washington

The purpose of this study was to measure how ^{18}F-FDG PET standardized uptake values (SUVs) change over time in breast cancer and to examine the feasibility of a method to adjust for modest variations in the time of uptake measurement experienced in clinical practice. **Methods:** ^{18}F-FDG PET was performed as 60-min dynamic imaging with an additional image acquired at ~75 min after injection. For 20 newly diagnosed, untreated, locally advanced breast cancer patients, both the maximum SUV and the average SUV within the lesion were calculated with and without correction for blood glucose concentration. A linear regression analysis of the portion of the time–activity curves starting at 27 min after injection was used to estimate the rate of SUV change per minute during the interval from 27 to 75 min. The rate of SUV change with time was compared with the instantaneous SUV obtained at different times from 27 to 75 min. **Results:** In untreated breast cancer, ^{18}F-FDG SUV values changed approximately linearly after 27 min at a rate ranging from −0.02 to 0.15 per minute. In addition, the rate of SUV change was linearly correlated with the instantaneous SUV measured at different times after injection (r^2 ranged from 0.82 to 0.94; $P < 0.001$). Using this information, an empirical linear model of SUV variation with time from injection to uptake measurement was formulated. The comparison method was then applied prospectively to a second set of 20 locally advanced breast cancer lesions not included in the initial analysis. The average percent error using the method to adjust for time differences was 8% and 5% for maximum SUVs and average SUVs ranging from 2 to 12. **Conclusion:** In untreated breast cancer, the SUV at any time point approximately predicts the rate of change of SUV over time. A comparison method based on this finding appears feasible and may improve the usefulness of the SUV by providing a means of comparing SUV acquired at different times after injection.

Key Words: standardized uptake value; ^{18}F-FDG; breast cancer; PET

J Nucl Med 2003; 44:1044–1050

The standardized uptake value (SUV) is a relative measure of tracer uptake in tissue used in ^{18}F-FDG PET (*1*). As pointed out by Keyes (*2*), the SUV varies with body habitus, plasma glucose concentration, and, perhaps one of the most important factors affecting the SUV, the time from injection to imaging. However, the SUV is a clinically practical and useful approach to tissue uptake quantification for diagnosis and treatment follow-up (*3*–*6*). Hamburg et al. (*7*) examined the temporal changes in SUV in 8 patients with stage III lung cancer and found a wide variation with time of measurement. Most PET centers allow for 40–70 min from injection to imaging (*8*). In a busy PET department, a fixed 45- or 60-min protocol can be difficult to adhere to precisely, and this may affect the SUV used for clinical interpretation. This is especially important in serial scan comparisons to measure tumor response to therapy. Understanding how SUV changes in tumors over time after injection is useful for comparing varying times between injection and PET imaging, thus improving the usefulness of ^{18}F-FDG SUV when comparing different studies, including serial studies in the same patient.

The purpose of this study was to measure how the SUV changes with observation time after injection in breast cancer and to examine the feasibility of an approximate method to compare the SUVs from studies with modest variations in the time between injection and uptake measurement experienced in clinical practice. Thie et al. (*8*) used dynamic scans of normal tissue and a heterogeneous group of tumors to explore the change in activity over time and to better define the appropriate time for imaging after injection based on optimal contrast ratios. They also suggested a method for correcting uptake measurements to a standardized time. Our study differs in that we analyzed dynamic scans of a homogeneous group of tumors and we also evaluated the potential error of this approach using a second independent study.

MATERIALS AND METHODS

^{18}F-FDG PET data from 20 newly diagnosed, untreated, locally advanced breast cancer patients were retrospectively analyzed. These patients were imaged as part of an ongoing study evaluating

Received Nov. 1, 2002; revision accepted Mar. 21, 2003.

For correspondence or reprints contact: David A. Mankoff, MD, PhD, Division of Nuclear Medicine, Box 356113, University of Washington Medical Center, 1959 N.E. Pacific St., Seattle, WA 98195.

E-mail: dam@u.washington.edu

PET imaging and locally advanced breast cancer at our institution. Results from some of these patients have been reported (*9*).

^{18}F-FDG PET imaging was performed using 246–393 MBq (6.7–10.6 mCi) ^{18}F-FDG, prepared using the method of Hamacher et al. (*10*). In all cases, ^{18}F-FDG radiochemical purity was >95% and specific activity was >47 GBq/μmol. ^{18}F-FDG was infused using a volume of 7–10 mL over 2 min in the antecubital vein contralateral to the affected breast. All imaging studies were performed using an Advance PET scanner (General Electric Medical Systems) operating in a 2-dimensional high-sensitivity mode with 35 imaging planes covering an axial field of view of 15 cm (4.0-mm axial full width at half maximum at the center of the tomograph) and an intrinsic in-plane resolution of ~5 mm (*11,12*). Before the PET study, patients fasted for a minimum of 6 h and blood glucose levels were measured using a glucose analyzer (Beckman Coulter, Inc.) before ^{18}F-FDG injection.

Dynamic imaging was performed for 60 min after the start of ^{18}F-FDG infusion. For the portion of the scans evaluated in this study, 5-min time bins were used. For 13 of the patients, a 7-min static emission scan, taken as part of a torso survey and starting up to 12 min after the 60-min dynamic study (yielding time points of up to 75 min), was also available and used for data analysis. Imaging data underwent corrections for attenuation, random coincidences, and scattered coincidences and were reconstructed into 35 transverse image planes (128 × 128 pixels) using filtered backprojection with a Hann 10-mm smoothing window. Image count data were converted to kilobecquerels/milliliter using data from calibration vials of known activity measured in a dose calibrator (radioisotope calibrator CRC-7; Capintec, Inc.).

For each lesion, the SUV versus time curves were generated using both the maximum SUV (S_{max}) and the average SUV (S_{av}) within a volume of interest (VOI). The VOI consisted of 3 circles of 17 pixels and ~1.5-cm diameter each, over 3 contiguous transaxial planes, each 4.5-mm thick, and the middle slice containing the maximum pixel value for the lesion. Both the S_{max} and the S_{av} were calculated using the formula:

$$S = \frac{A_{VOI}}{ID/W}, \qquad \text{Eq. 1}$$

where A_{VOI} is the measured activity in the VOI (in μCi/mL), ID is the injected dose (in mCi), and W is the body weight of the patient (in kg). SUVs were also processed with correction for blood glucose concentration by using the formula (*13*):

$$S_{Glu} = S \cdot \frac{[Glu]}{100}, \qquad \text{Eq. 2}$$

where S_{Glu} is the glucose-corrected SUV and [Glu] is the blood glucose level (in mg/dL). Because this study examined the change in SUV with time of uptake, all tumors were >2 cm, and the regions of interest were 1.5 cm in diameter, no partial-volume correction was applied.

The time of each SUV was considered to be the midinterval of each acquisition time bin or frame. As mentioned above, for most studies, an additional SUV measurement was obtained between 71 and 75 min after injection from a subsequent standard clinical scan.

A linear regression analysis of the curves after 27 min following injection was used to estimate the rate of SUV change (dS/dt [min^{-1}]) during the interval from 27 to 75 min for each lesion. The estimated dS/dt was compared with the instantaneous measured SUV at 27, 42, 57, and 75 min after injection. Using a linear model of dS/dt versus SUV(t), an empirical method for comparing SUV for varying times from injection to uptake measurement based on the linear correlation of dS/dt versus SUV(t) was formulated.

To test the validity of this comparison method, we selected a second set of 20 locally advanced breast cancer lesions in patients not included in the initial analysis who were studied using the same the same imaging protocol and data analysis as described above. Using the comparison method based on our linear model, we estimated the S_{max} and S_{av} at 71–75 min after injection using the known S_{max} and S_{av} at 45 min in those patients. The estimated values were compared with the measured values at 71–75 min.

RESULTS

Patients and Tumors

The 20 patients studied included 6 whose findings were reported in our prior analysis of blood flow and metabolism determined by PET (*9*). Patients ranged from 33 to 72 y old (mean, 49 y) at the time of their study participation. Of the 20 patients, 13 were premenopausal women. Blood glucose level at the time of injection ranged from 74 to 117 mg/mL (mean, 88 mg/mL). The size of the breast lesions ranged from 2 to 11 cm in diameter (mean, 6 cm) as assessed by mammography, ultrasound, or physical examination conducted before therapy. Histopathologic analysis of core needle biopsy specimens revealed 16 infiltrating ductal carcinomas (11 low grade, 5 intermediate grade) and 4 infiltrating lobular carcinomas (1 intermediate grade, 3 high grade). Three of the 20 patients had inflammatory breast cancer at the time of diagnosis.

SUV Measurements

Figure 1 shows the tumor time–activity curves of tumor VOIs for all patients. At 57 min, the S_{max} for the tumors ranged from 1.3 to 12.4 (mean, 6.6) and the S_{av} ranged from 0.9 and 10.6 (mean, 4.9). When blood glucose correction was applied, the S_{max} at 57 min ranged from 1.0 to 10.5 (mean, 5.8) and the S_{av} ranged from 0.7 and 8.6 (mean, 4.3).

Rate of Uptake Change with Time

Linear regression analysis was applied to each of the curves in Figure 1 starting at 27 min. Figure 2 shows examples of linear fits for 2 lesions, one for which the linear regression generated a positive slope (Fig. 2A) and another for which the linear regression generated a negative slope (Fig. 2B). As illustrated by these curves (Figs. 1 and 2), S_{max} showed more variability than S_{av}. This is most likely due to a higher statistical noise for S_{max} compared with S_{av}. ^{18}F-FDG uptake changed approximately linearly between 27 and 75 min. The dS_{max}/dt (slope of the linear regression) ranged from −0.02 to 0.15 min^{-1} and was positive (increased uptake over time) for 17 patients and negative (decreased uptake over time) for 3 patients. The dS_{av}/dt ranged from −0.02 to 0.12 min^{-1} and was positive for the same 17 patients and negative for the same 3 patients as for S_{max}. Because the shapes of the curves did not change after blood glucose correction, the linear regression results are similar with and without blood glucose correction.

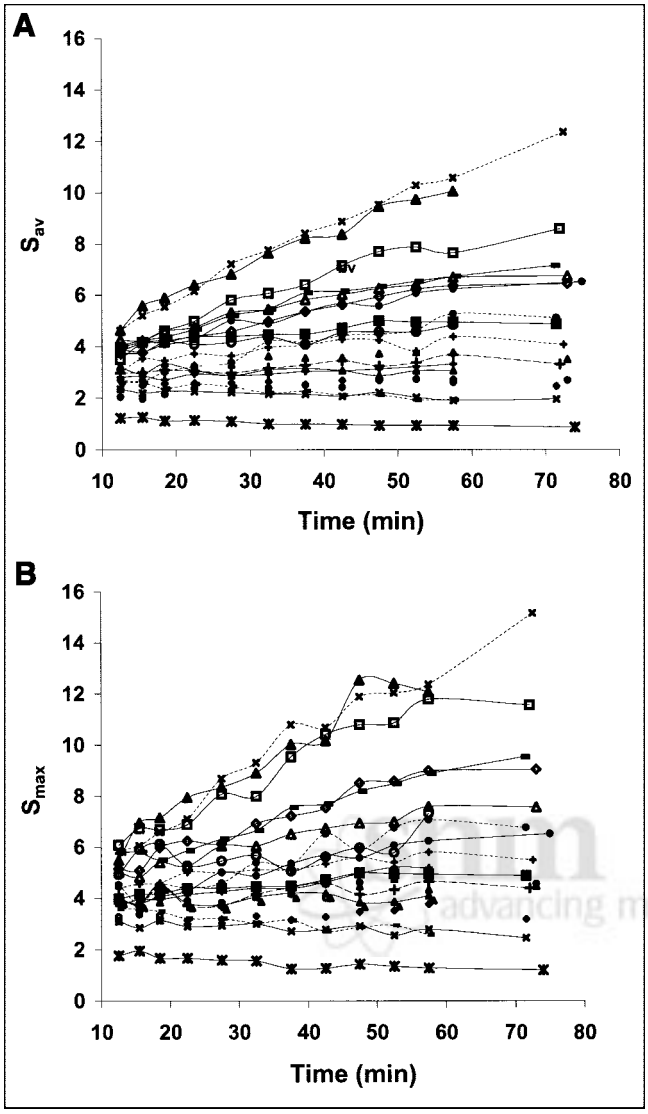

FIGURE 1. Tumor time–activity curves of VOIs for all patients: S_{av} (A) and S_{max} (B) vs. time.

Correlation of Rate of SUV Change with SUVs at Different Times After Injection

Table 1 displays correlation results between the rate of SUV change and SUVs measured at different times after injection, with and without blood glucose correction applied. Figure 3 shows graphically the correlation result at 57 min after injection for the S_{av} without glucose correction. These findings suggest that the rate of SUV change over time can be approximately predicted from an instantaneous SUV measured at 27–75 min with a simple linear model. The correlations were slightly better for the SUV at later time points. In other words, the rate of SUV change was more accurately predicted as the time from injection increased.

Linear Model and Approximate Comparison Method

Assuming a linear increase in SUV over time we have:

$$\tilde{S}_2 = S_1 + (t_2 - t_1) \cdot dS/dt, \qquad \text{Eq. 3}$$

where $\tilde{S}_2$ is the estimated SUV at a desired time t_2, S_1 is the measured SUV at time t_1, and dS/dt is the rate of SUV change at the measurement time t_1 for SUV, S_1. The value for dS/dt can be obtained from the plots of the linear fits of dS/dt versus S in Figure 4 for the measurement time, t_1.

Alternately, if we also assume that at a fixed reference time, t_0, the rate of change depends linearly on the SUV at that time, t_0, then:

$$dS/dt = a + bS_0, \qquad \text{Eq. 4}$$

where a and b are intercept and slope constants. These constants were estimated from the measured data and are listed in Table 1 for different reference times (t_0). In the range of approximate linear behavior there is only 1 line that connects (S_1, t_1) and (S_2, t_2) (Fig. 5). This line will also have a unique value S_0 at the reference time t_0, for which the

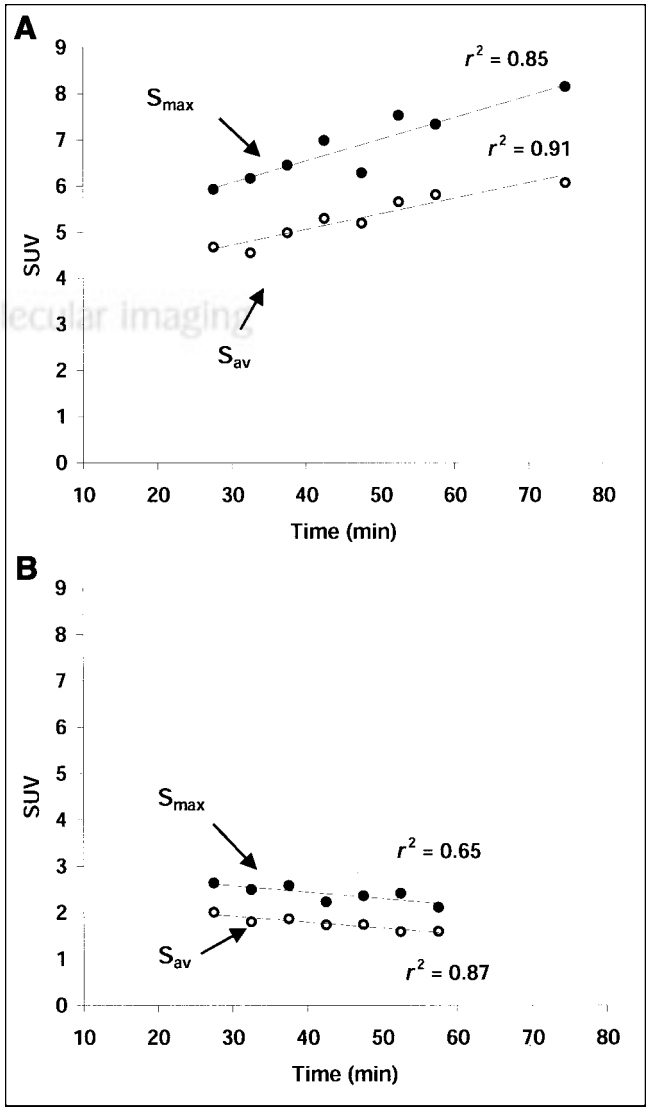

FIGURE 2. Example of linear fit for 2 lesions, one for which linear regression generated positive slope (A) and another for which linear regression generated negative slope (B).

TABLE 1
Linear Correlation Regression Results (Eq. 4) for SUV Rate of Change vs. SUVs at Different Reference Times (t_0)

Without glucose correction				With glucose correction			
t_0 (min)	Slope (*b*)	Intercept (*a*)	r^{2*}	t_0 (min)	Slope (*b*)	Intercept (*a*)	r^{2*}
Average SUV							
27	0.020	−0.050	0.82	27	0.020	−0.050	0.82
42	0.015	−0.042	0.87	42	0.015	−0.034	0.84
57	0.013	−0.036	0.92	57	0.012	−0.030	0.89
71–75	0.010	−0.026	0.94	71–75	0.010	−0.023	0.92
Maximum SUV							
27	0.022	−0.070	0.87	27	0.022	−0.070	0.87
42	0.016	−0.054	0.88	42	0.015	−0.041	0.82
57	0.014	−0.049	0.90	57	0.013	−0.038	0.86
71–75	0.011	−0.033	0.94	71–75	0.010	−0.028	0.91

*$P < 0.001$ for all.

slope of the line is known (Eq. 4 and Table 1). Because $dS/dt = a + bS_0 = (S_1 - S_0)/(t_1 - t_0)$, straightforward rearrangement leads to $S_0 = (S_1 - a[t_1 - t_0])/(1 + b[t_1 - t_0])$, thus:

$$dS/dt = a + b\left(\frac{S_1 - a[t_1 - t_0]}{1 + b[t_1 - t_0]}\right). \qquad \text{Eq. 5}$$

This can be used with Equation 3 to estimate the SUV at any other time in the range of approximate linear behavior. For example, a tumor having a glucose-corrected S_{max} of 9.0 at 42 min will have a 0.11 min^{-1} rate of S_{max} change over time, dS_{max}/dt (given by Eq. 5 and by *a* and *b* in Table 1), and the estimated S_{max} for comparison at 72 min will be ~12.3. We note that, in principle, any reference time can be used for the values *a* and *b*. Alternately, the approximate value for dS/dt can be found graphically using Figure 4.

Figure 6 shows the results of testing our method on a second, independent set of 20 locally advanced breast cancer lesions in patients not included in the initial analysis and imaged using the same protocol. The estimated S_{max} ($\tilde{S}_2$) at

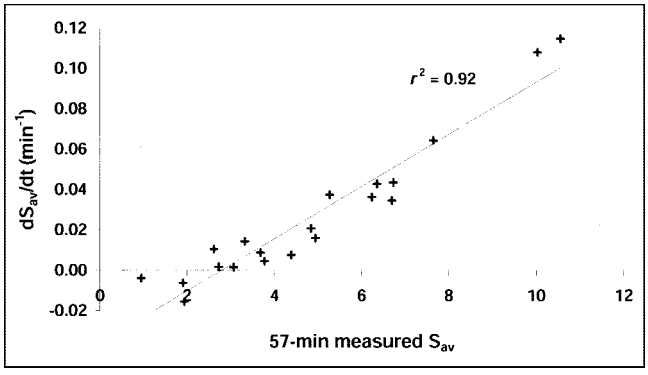

FIGURE 3. Rate of average S_{av} change vs. measured S_{av} at 57 min. SUV measurements were not corrected for plasma glucose concentrations.

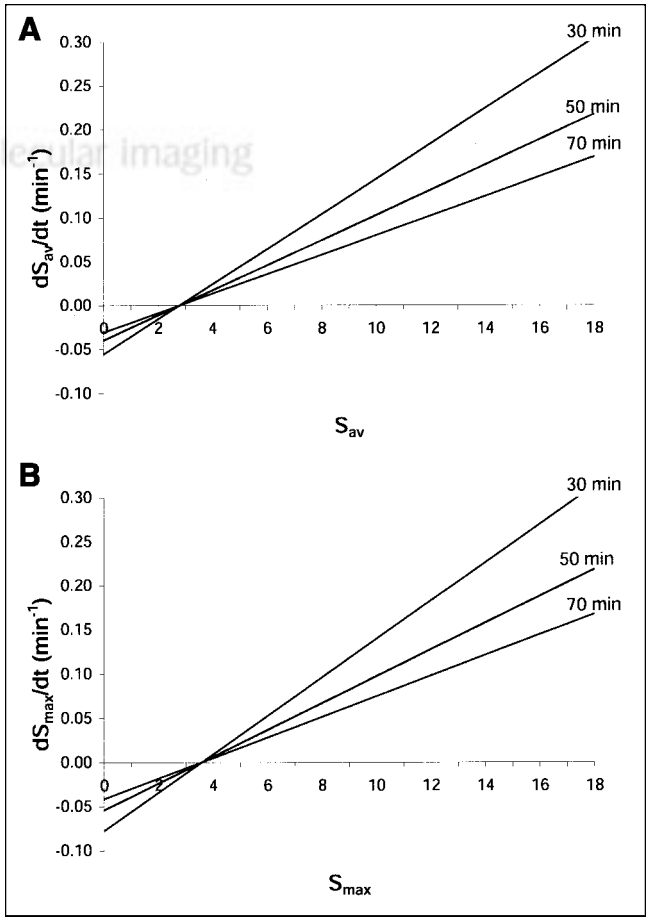

FIGURE 4. Rate of SUV change vs. SUV at single time point for different single uptake time points: glucose-corrected S_{av} (A) and glucose-corrected SUV_{max} (B). These plots can be used to compare SUV measured at different times between studies.

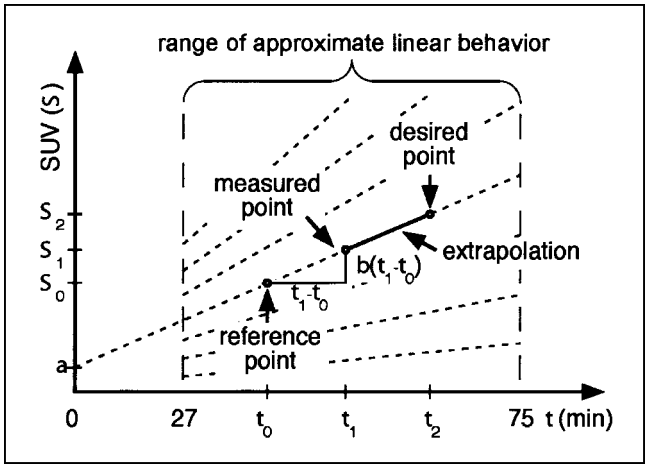

FIGURE 5. Illustration of proposed SUV correction method where SUV increases linearly with time, and rate of change (dS/dt) at any fixed time increases linearly with SUV value (S) at that time (dashed lines). From any measured point, a desired point can be extrapolated by use of a predetermined reference point as given in Equations 3 and 5 and Table 1.

71–75 min after injection using the comparison method at a reference time (t_0) equal to 57 min and a measured S_{max} (S_1) at 45 min (t_1) was compared with the measured S_{max} at 71–75 min. Table 2 shows the average percent error on the S_{max} and S_{av} measured at 71–75 min. The comparison method was most accurate for SUVs (both S_{max} and S_{av}) higher than 5. For SUVs lower than 5, the comparison method had an average percent error comparable to simply ignoring the effect of differences in injection time. As expected, the method performed better (lower average percent error) using S_{av} due the significantly higher intrinsic statistical noise of S_{max} as compared with S_{av}.

DISCUSSION

We described the SUV change over time after injection up to 75 min in locally advanced breast cancer. These tumors exhibit a wide range of ^{18}F-FDG uptake, as reported (*9*). Within the 27- to 75-min time interval, however, we found 2 levels of approximate linearity. First, we found that the ^{18}F-FDG change over time was approximately linear or, at least, that a linear model would be good enough within the specific interval to be used as a basis for our comparison method. We emphasize that the overall time–activity curves of ^{18}F-FDG uptake are not linear. The behavior in the time interval from approximately 27–75 min, however, was well described by a linear fit in all 40 cases studied. As a second level of linearity, we found that the level of ^{18}F-FDG uptake and the rate of change in ^{18}F-FDG uptake over time are approximately linearly correlated. Tumors with low uptake can have SUVs that increase little with time or even decrease slightly, whereas tumors with high uptake can have a 20%–25% increase in SUV in only 15 min. This could be a significant confounding factor for using ^{18}F-FDG PET to follow response to therapy if injection to imaging time varied. Thie et al. (*8*) pointed out that sequential scans should be compared on the basis of the midpoint of the acquisition duration (frame). This applies to both dynamic (single bed position) and whole-body (multiple bed positions) studies, where there can be a significant difference between the start and end times. We agree that this is important, given the magnitude of SUV change over time observed with breast cancer in our study.

It is notable that some tumors in our series with lower metabolic activity undergo a small decline in SUV over time. This could potentially confound dual time point imaging protocols used to distinguish a tumor from inflammatory or benign processes (*14,15*), because some tumors with lower uptake may have a late uptake-to-early uptake ratio less than unity and would be falsely considered benign.

The wide variation in SUV change among locally advanced breast cancer stresses the importance of consistently acquiring images at the same time after injection. However, in a busy PET service, this is not always possible to achieve. A literature survey of articles published since 1990 was conducted that showed considerable variability of SUV measurement time after injection even within protocols at the same institution (*8*). A corrective method to standardize the time of SUV estimation would increase the clinical usefulness of SUVs.

The strong linear correlation between the rate of SUV change and the SUV measured at different times after injection is in accordance with the findings of Thie et al. (*8*), who suggested that more metabolically active tissues can show steeper time–activity curve slopes. This information can be used to compare the SUV for varying times of uptake by using the linear model and Equation 3. The approach proposed here using Equations 3 and 5 (or Fig. 4) can be

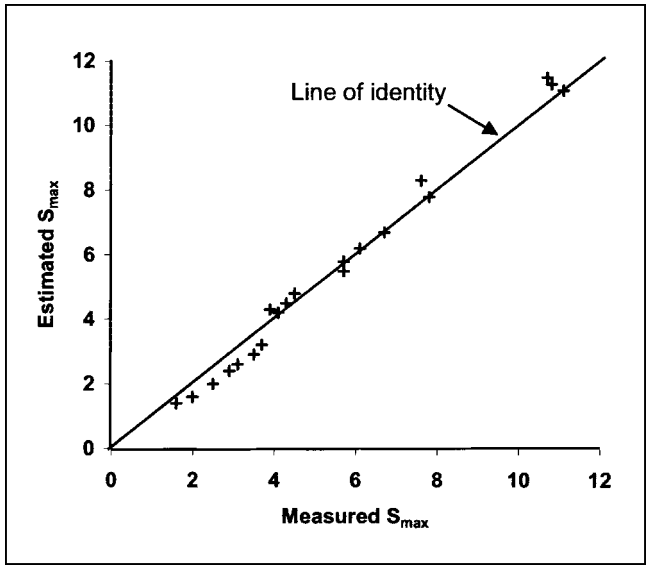

FIGURE 6. Estimated S_{max} at 71–75 min after injection (using Eq. 3) compared with measured value at 71–75 min for 20 additional locally advanced breast cancer lesions in patients not included in original analysis.

TABLE 2
Average Percent Error

Parameter	Without correction method			With correction method		
	All SUVs (n = 20)	SUVs < 5 (n = 13)	SUVs > 5 (n = 7)	All SUVs (n = 20)	SUVs < 5 (n = 13)	SUVs > 5 (n = 7)
S_{max}	11	8	15	8	12	3
S_{av}	8	6	12	5	7	2

used as a simple tool to compare SUV for imaging time variations and to guide clinical interpretation of SUV. The linear model was validated for SUV from 2 to 12 measured between 27 and 75 min and, thus, our method may not apply to tumors with SUVs outside this range or with injection to scan time outside of the specified interval. As shown by the average percent error (Table 2), the comparison method is more useful for SUVs in the upper range (>5) and performed better using the S_{av} as compared with the S_{max}. For SUVs in the lower range (<5), the rate of SUV change over time and, thus, the absolute SUV change will be small and adjustment using our method is unnecessary. The accuracy of this comparison method also depends on the uncertainty on SUV measurements, which is larger, while using S_{max} as compared with S_{av}.

Some additional sources of variability need to be considered in applying the proposed comparison method. If the method were to be used with tumors of <2 cm in size, underestimation of the SUV due to partial-volume averaging would lead to underestimation of the rate of SUV change over time. Similar to the glucose correction, the use of a different normalization factor (lean body weight or surface area) would simply rescale the SUV versus time curve on the *y*-axis in a given patient without changing the shape of the curve. Therefore, a similar empirical linear model could be applied to SUV normalized with lean body weight or surface area.

Our model assumes that the SUV curves are approximately linear within the specified time interval. However, the shapes of SUV curves may be different for other types of tumors, which will affect the approximation. For example, tumors having a significant FDG dephosphorylation rate may have significant deviation from linearity of their SUV curves within the time interval studied. Similarly, the shapes of SUV curves may change after treatment (as shown in lung cancer (*7*)). Consequently, our comparison method may not necessarily apply to tumor types other than breast cancers or to treated breast tumors.

Future studies should examine SUV time dependency in a variety of treated and untreated tumors to refine such a comparison method. Also, studies using kinetic analysis in breast cancer may be helpful to understand the underlying biologic characteristics that explain the 2 levels of approximate linearity observed in our study in the specified time interval.

CONCLUSION

Given the magnitude of SUV change over time in untreated, locally advanced breast cancer, variations in time after ^{18}F-FDG injection can be a major confounding factor for patient-to-patient comparisons and follow-up comparisons for a single patient. The time dependency of ^{18}F-FDG SUV (*7*) stresses the importance of consistently acquired images at the same time after injection. However, if this cannot be achieved in a busy PET department, an empirical SUV comparison method to adjust for differences in the time of uptake based on a linear model appears feasible. More studies are needed before this method can be applied to other tumors, treated tumors, or imaging time beyond 75 min.

ACKNOWLEDGMENTS

The authors acknowledge the support of the University of Washington Radiochemistry Group for isotope production; Dr. Thomas Lewellen and Mr. Steven Kohlmeyer for tomograph support; University of Washington PET technologists for technical assistance with the imaging studies; Dr. Janet Eary and Kenneth Krohn for helpful comments; Mimi Shurts for patient care coordination; the late Dr. Aaron Charlop for long-time collaboration; and the physicians and staff of the University of Washington Breast Cancer Specialty Clinic for help with patient referrals. This study was supported by National Institutes of Health grants CA72064, CA42045, and CA74135.

REFERENCES

1. Huang SC. Anatomy of SUV. *Nucl Med Biol.* 2000;27:643–646.
2. Keyes JW. SUV: standard uptake or silly useless value? *J Nucl Med.* 1995;36:1836–1839.
3. Delbeke D, Rose DM, Chapman WC, et al. Optimal interpretation of FDG PET in the diagnosis, staging and management of pancreatic carcinoma. *J Nucl Med.* 1999;40:1784–1791.
4. Watanabe H, Shinozaki T, Aoki J, et al. Glucose metabolic analysis of musculoskeletal tumors using fluorine-18-FDG PET as an aid in preoperative planning. *J Bone Joint Surg [Br].* 2000;82:760–767.
5. Rinne D, Baum RP, Hor G, Kaufmann R. Primary staging and follow-up of high risk melanoma patients with whole-body ^{18}F-fluorodeoxyglucose positron emission tomography: results of a prospective study of 100 patients. *Cancer.* 1998;82:1664–1671.
6. Schelling M, Avril N, Nahrig J, et al. Positron emission tomography using [^{18}F]fluorodeoxyglucose for monitoring primary chemotherapy in breast cancer. *J Clin Oncol.* 2000;18:1689–1695.
7. Hamburg LM, Hunter GT, Albert NM, et al. The dose uptake ratio as an index of glucose metabolism: useful parameter or oversimplification? *J Nucl Med.* 1994;35:1308–1312.

8. Thie JA, Hubner KF, Smith GT. Optimizing imaging time for improved performance in oncology PET studies. *Mol Imaging Biol.* 2002;4:238–244.
9. Mankoff DA, Dunwald LK, Gralow JR, et al. Blood flow and metabolism in locally advanced breast cancer: relationship to response to therapy. *J Nucl Med.* 2002;43:500–509.
10. Hamacher K, Coenen HH, Stocklin G. Efficient stereospecific synthesis of no-carrier-added 2-[^{18}F]-fluoro-2-deoxy-D-glucose using aminopolyether supported nucleophilic substitution. *J Nucl Med.* 1988;29:241–247.
11. DeGrado TR, Turkington TG, Williams JJ, Stearns CW, Hoffman JM, Coleman RE. Performance characteristics of a whole body PET scanner. *J Nucl Med.* 1994;35:1398–1406.
12. Lewellen TK, Kohlmeyer S, Miyaoka R, Schubert S, Stearns C. Investigation of the count rate performance of the General Electric Advance positron emission tomograph. *IEEE Trans Nucl Sci.* 1995;42:1051–1057.
13. Eary JF, Mankoff DA. Tumor metabolic rates in sarcoma using FDG PET. *J Nucl Med.* 1998;39:250–254.
14. Hustinx R, Smith RJ, Benard F, et al. Dual time point fluorine-18 fluorodeoxyglucose positron emission tomography: a potential method to differentiate malignancy from inflammation and normal tissue in the head and neck. *Eur J Nucl Med.* 1999;26:1345–1348.
15. Matthies A, Hickeson M, Cuchiara A, Alavi A. Dual time point ^{18}F-FDG PET for the evaluation of pulmonary nodules. *J Nucl Med.* 2002;43:871–875.